BIOCHEMISTRY
including biophysical chemistry & molecular biology
Rapid Report

Biochemistry **2009,** *48,* 9949–9951 9949
DOI: 10.1021/bi901166n

Simulations of the BM2 Proton Channel Transmembrane Domain from Influenza Virus B[†]

Sarah L. Rouse,[‡] Timothy Carpenter,[§] Phillip J. Stansfeld,[‡] and Mark S. P. Sansom*[,‡]

[‡]*Department of Biochemistry, University of Oxford, Oxford OX1 3QU, U.K., and* [§]*Lawrence Livermore National Laboratory, Livermore, CA 94550*

Received July 9, 2009; Revised Manuscript Received September 13, 2009

ABSTRACT: BM2 is a small integral membrane protein from influenza B virus which forms proton-permeable channels. Coarse-grained (CG) molecular dynamics simulations have been used to produce a model of the BM2 channel by self-assembly of a tetrameric bundle of BM2 transmembrane helices in a lipid bilayer. The BM2 channel model is conformationally stable on a 5 μs time scale. This CG model was converted to atomistic resolution to refine interhelix and channel−water interactions. Atomistic molecular dynamics simulations indicate that the BM2 channel is closed when no more than two of the four His19 residues are protonated. Protonating a third His19 side chain initiates a conformational change that opens the channel. In summary, our simulations suggest a common mechanism for BM2 and A/M2, whereby changes in helix packing play a functional role in channel gating.

Influenza A and B viruses contain small integral membrane proteins that are vital for viral replication. The A/M2 and BM2 proteins are proton-selective channels that at low external pH allow protons to pass through the viral membrane (*1*). The ensuing acidification of the interior of the virus particle results in uncoating of the virion and allows genetic material to replicate. The A/M2 protein has been studied extensively by both experimental and computational approaches. BM2 is less well understood but remains of interest, especially because influenza B almost exclusively infects humans.

BM2 consists of a seven-residue N-terminal ectodomain, a transmembrane (TM)[1] domain region of 19 amino acid residues, and a large cytoplasmic domain of 83 residues (*2*). The BM2 channel functions like A/M2 despite the only sequence homology being the HxxxW motif (*1*). Mutagenesis studies indicate that this motif is responsible for the gating mechanism of both A/M2 and BM2.

Several three-dimensional structures have been determined for the A/M2 channel (*3*, *4*). The BM2 channel is structurally less well characterized. As for A/M2, BM2 functions as a homotetramer, with the TM domain responsible for oligomerization (*5*). The pore-lining residues of the TM region correspond to those predicted from sequence alignment of the HxxxW motif (*6*) The TM peptide from BM2 is able to form functional channels, and π-cation interactions in the HxxxW motif may be involved in the channel opening mechanism (*7*).

A key difference between the two M2 channels is that A/M2 is found to be inhibited by amantadine and related antiviral drugs whereas BM2 is not (*1*). It is therefore of interest to model the BM2 channel to compare its structure−function relationships to those of A/M2.

Coarse-grained molecular dynamics (CGMD) simulations, in which groups of approximately four heavy (non-hydrogen) atoms are replaced with a single, larger particle, have been used recently to study self-assembly of the influenza A/M2 tetramer (*8*). The reduced complexity of CGMD systems allows much larger (> 1 μs) simulation time scales to be readily achieved.

We have used CGMD to self-assemble a model of the BM2−TM tetramer. This model is then converted to an atomistic representation to explore a possible mechanism of channel opening via protonation of His19 residues. CGMD TM helix insertion and tetramerization simulations are fully described in the Supporting Information. A 27-mer peptide (P^4FQILSICSFILSALHFMAWTIGHLNQ^{30}) was used to model the putative TM domain of BM2 in an α-helical conformation (restrained to be α-helical during CGMD simulations), with three residues on either side of the helix in a random coil configuration. An atomistic model was built and converted to a CG model using a previously described protocol (*8*).

In the single-TM helix insertion simulations, a single BM2 helix was positioned in a box with 256 randomly placed and oriented CG dipalmitoylphosphatidylcholine (DPPC) lipids, along with ∼3000 CG water particles and eight CG Cl^- ions. The system was simulated for 0.2 μs. This initial simulation resulted in a stable bilayer with the BM2 helix adopting a transmembrane orientation (see Figure S1). The single inserted helix was then replicated to give four monomers inserted in parallel fashion ∼45 Å from each other. This system was the basis for five independent CG tetramerization simulations, each 5 μs in duration.

The formation of helix bundles was monitored using the distance between the centers of mass of the Cα particles of pairwise combinations of helices (see Figure S2). In each case, the tetramer was seen to form via a dimer or trimer, with initial formation of a loose tetrameric assembly which subsequently formed a left-handed bundle of approximate 4-fold symmetry. The average time to tetramer formation was 0.5 ± 0.2 μs. The first 1 μs of the simulation was discarded as equilibration time. The remaining 4 μs of each simulation was clustered to generate the top three representative frames from each simulation (Figure 1). Comparison of these 15 structures yielded a single converged CG model of the BM2−TM tetramer.

In each of the CGMD simulations, the helices packed together to form a left-handed tetramer with an average tilt angle of

[†]This work was supported by the BBSRC and the Wellcome Trust.

*To whom correspondence should be addressed: Department of Biochemistry, University of Oxford, South Parks Road, Oxford OX1 3QU, U.K. E-mail: mark.sansom@bioch.ox.ac.uk. Phone: 44-1865-613306. Fax: 44-1865-613238.

[1]Abbreviations: CGMD, coarse-grained molecular dynamics; ATMD, atomistic molecular dynamics; TM, transmembrane; rmsd, root-mean-square deviation.

Published on Web 09/25/2009

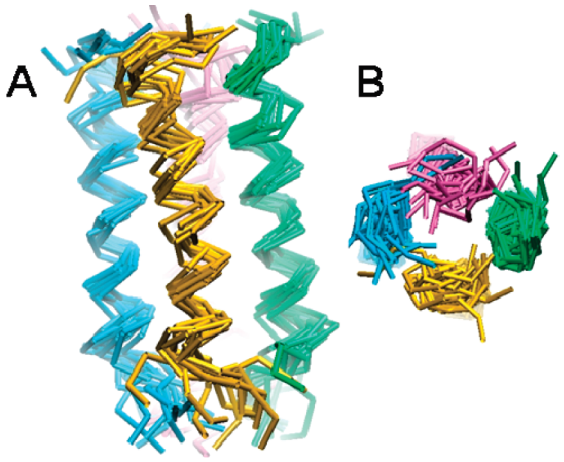

FIGURE 1: Overlay of representative frames from five independent CGMD tetramerization simulations.

$13 \pm 3°$ and crossing angles between sequential helices of $14 \pm 4°$. The orientation of helices within the tetramer was such that the proposed pore-lining residues (Ser9, Ser12, Ser16, His19, and Trp23) were indeed facing the center of the bundle. The bundle displays approximate 4-fold symmetry. The helices are packed together more tightly at the N-terminal region than at the C-terminal region where large Trp23 particles must be accommodated.

To investigate a possible mechanism of channel gating, the BM2−TM complex was converted to an atomistic representation to allow conventional atomistic MD (ATMD) simulations to be performed. As mentioned previously, at low pH the channel is able to open and transport protons across the virus membrane. Previous studies of A/M2 have linked channel opening at low pH to protonation of the His37 residue. Similarly, the homologous residue in BM2, His19, is the only ionizable side chain within the TM domain and has been found to be vital for the channel to function; therefore, it is probable that channel opening coincides with protonation of this residue. ATMD is more suitable than CGMD for studying protonation effects and water behavior in the pore.

The model generated from CGMD tetramerization simulations was converted to an atomistic system, using a fragment-based approach. Initially, the CG model of the BM2 tetramer in the +2 state (with two His19 residues on adjacent chains protonated) was converted to an atomistic model (AT-2+). The CG bilayer was also converted, and water and Cl^- counterions were added. During the ATMD simulation, the protein was restrained for 2 ns while the lipids were allowed to relax around it. Following this, the positional restraints were removed and a 30 ns production run was performed. This tetramer (AT-2+) was shown to be stable with a Cα rmsd for the α-helical residues of ~2.6 Å during the simulation (see Figure S3). These initial simulations of AT-2+ suggested that the BM2 channel with two of the four His19 residues protonated was closed. We therefore decided to focus on consecutive protonation steps of His19 residues. To explore how protonation might lead to channel opening, we simulated a triply protonated system (AT-3+) followed by protonation of all four His19 residues (AT-4+).

Pore profile analysis conducted with representative frames from the last 10 ns of the AT-2+ simulation identified a constriction in the putative gating HxxxW region such that no water molecules were able to pass (Figure 2). Protein−protein contact analysis showed that the main interhelix contacts occur

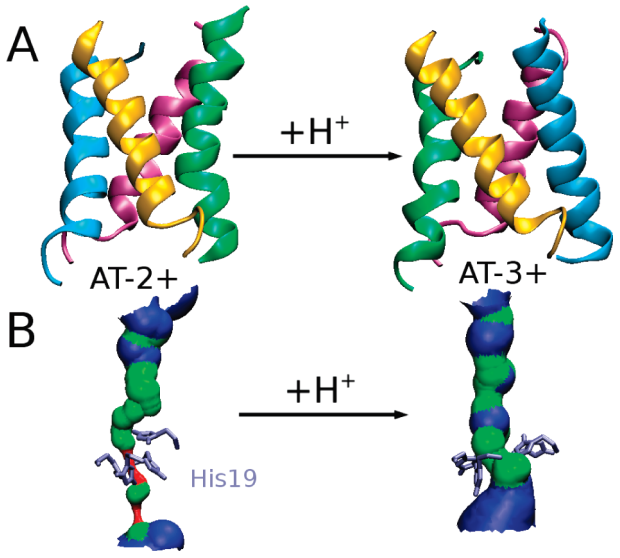

FIGURE 2: (A) Representative structures from the AT-2+ (left) and AT-3+ (right) ATMD simulations. Only the α-helical region is shown for the sake of clarity. (B) Pore lining surfaces highlighting the constriction in the HxxxW gating region in the AT-2+ model, which is no longer observed in the AT-3+ structure.

between the tightly packed pore-lining serine residues in the N-terminal region. These interact in a predominantly dimer−dimer manner.

A representative frame from the last 10 ns of this simulation was used to generate a model of the triply protonated (AT-3+) state. A 30 ns simulation was performed to assess the effect of a third protonated His19 residue on the tetramer structure and dynamics of waters in the pore. The additional charge on the His19 residue caused the helices to move apart, with a Cα rmsd of ~1.7 Å over the 30 ns simulation. Pore profile analysis of the last 10 ns demonstrated that the constriction at HxxxW was removed but that most of the Ser−Ser contacts were conserved. In the AT-3+ simulation, the Trp side chains reorient so that they no longer occlude the pore. This appears to be due to H-bond interactions with Trp being lost while new interactions form, in particular between Trp23 and Gln30 of an adjacent chain, to orient the Trp side chain away from the pore. Protein−solvent contact analysis demonstrated that the pore-lining residues of the AT-3+ system formed approximately twice as many contacts with water molecules over the final 10 ns of each simulation as for the AT-2+ system. A water molecule passed through the channel in one instance.

As a further step in the study of the effect of His19 protonation state, the final structure from the AT-3+ simulation used as a starting point for a switch to a 4+ state. All four His19 residues were protonated, and a production run (AT-4+) 30 ns in duration was performed. The increase in the level of electrostatic repulsion between charged His19 residues leads to a large conformational change (Cα rmsd ~ 4 Å) such that the helices are splayed apart at the C-terminal end, giving a more conical structure. The helices are prevented from drifting entirely apart by Ser−Ser contacts in the N-terminal region and a chloride ion coordinating to two of the protonated His19 residues. This conical structure resembles the X-ray structure [Protein Data Bank (PDB) entry 3C9J] of the A/M2 TM peptide, with a Cα rmsd of 3.6 Å for the overlapping residues. A comparison of the AT-2+ structure to the neutral-pH A/M2 NMR structure also gives a reasonable fit (Cα rmsd = 2.3 Å). Therefore, these

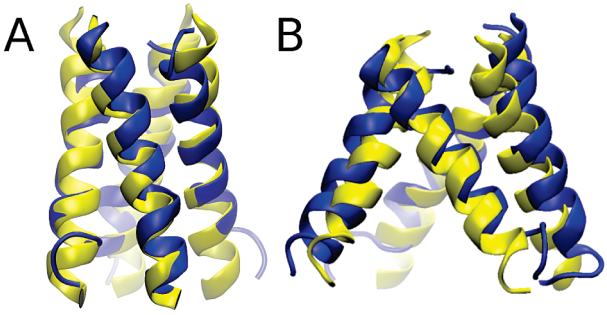

FIGURE 3: BM2 structures from ATMD (blue) and A/AM2 structures (yellow). (A) AT-2+ structure overlaid on the neutral-pH A/M2 NMR structure (PDB entry 2RLF). (B) AT-4+ structure overlaid on the X-ray structure of A/M2 (PDB entry 3C9J).

initial observations provide some evidence to suggest that ATMD simulations are able to replicate the conformational changes upon going from a neutral pH (closed channel) to a low pH [open channel (Figure 3)]. However, it is important to note that in the NMR structure an amphipathic C-terminal helix is also present whereas in the X-ray structure only the TM peptide is used. The C-terminal extension (not present in the BM2 model) may modulate the packing of the TM helices, as appears to be the case for A/M2.

These ATMD studies inform our understanding of the differing amantadine sensitivities of A/M2 and BM2. Pore-lining surfaces (see Figure S4) for BM2 exhibit a central cavity comparable in size to that in A/M2. This in turn suggests that dynamic changes in the geometries of these two pores may be responsible for their differing sensitivity to amantadine.

In conclusion, we have used CGMD to generate a stable model of the tetrameric BM2 TM peptide. ATMD has then been used to provide evidence that the BM2 proton channel is closed when no more than two of the four His19 residues are protonated and that protonating the third His19 residue leads to a conformational change that opens the channel. This agrees with NMR studies of A/M2 (*9*).

A possible limitation of this MD study is the fact that the proposed π-cation interactions within the HxxxW motif are not fully described by the ATMD force field. A further point to note is that the CGMD study demonstrates that the helix bundles are highly dynamic and therefore helix motions associated with protonation of His19 may occur on a time scale longer than the scale that can be observed with ATMD. Motions of pore-lining residues on a longer time scale may allow the formation of a water wire in the 2+ state. Further work could include modeling a C-terminal extension to see if this helps to anchor the tetramer together at the C-terminal domain.

We also used CGMD to explore formation of BM2 pentamers. Pentameric aggregates were formed but did not yield stable bundles of helices. This suggests further studies of CGMD simulations to define TM helix oligomerization states would be productive.

In summary, the behavior of BM2 in simulations seems to mimic aspects of structural and simulation (*10*−*12*) studies of A/M2 in that multiple packings of the helices occur, apparently modulated by changes in pH and environment. Conservation of such behavior between A/M2 and BM2 strengthens suggestions that changes in M2 helix packing may play a functionally relevant role in gating and/or transport by this small but far from simple channel protein.

SUPPORTING INFORMATION AVAILABLE

Further experimental details and figures. This material is available free of charge via the Internet at http://pubs.acs.org.

REFERENCES

1. Pinto, L. H., and Lamb, R. A. (2006) *J. Biol. Chem. 281*, 8997–9000.
2. Paterson, R. G., Takeda, M., Ohigashi, Y., Pinto, L. H., and Lamb, R. A. (2003) *Virology 306*, 7–17.
3. Schnell, J. R., and Chou, J. J. (2008) *Nature 451*, 591–595.
4. Stouffer, A. L., Acharya, R., Salom, D., Levine, A. S., Di Costanzo, L., Soto, C. S., Tereshko, V., Nanda, V., Stayrook, S., and DeGrado, W. F. (2008) *Nature 451*, 596–599.
5. Balannik, V., Lamb, R. A., and Pinto, L. H. (2008) *J. Biol. Chem. 283*, 4895–4904.
6. Ma, C. L., Soto, C. S., Ohigashi, Y., Taylor, A., Bournas, V., Glawe, B., Udo, M. K., DeGrado, W. F., Lamb, R. A., and Pinto, L. H. (2008) *J. Biol. Chem. 283*, 15921–15931.
7. Otomo, K., Toyama, A., Miura, T., and Takeuchi, H. (2009) *J. Biochem. 145*, 543–554.
8. Carpenter, T., Bond, P. J., Khalid, S., and Sansom, M. S. P. (2008) *Biophys. J. 95*, 3790–3801.
9. Hu, J., Fu, R., Nishimura, K., Zhang, L., Zhou, H. X., Busath, D. D., Vijayvergiya, V., and Cross, T. A. (2006) *Proc. Natl. Acad. Sci. U.S.A. 103*, 6865–6870.
10. Kass, I., and Arkin, I. T. (2005) *Structure 13*, 1789–1798.
11. Chen, H. N., Wu, Y. J., and Voth, G. A. (2007) *Biophys. J. 93*, 3470–3479.
12. Khurana, E., Dal Peraro, M., DeVane, R., Vemparala, S., DeGrado, W. F., and Klein, M. L. (2009) *Proc. Natl. Acad. Sci. U.S.A. 106*, 1069–1074.